ORIGINAL ARTICLE

Cancer Science WILEY

Cancer stem cells in Epstein-Barr virus-associated gastric carcinoma

Mariko Yasui[1,2] | Akiko Kunita[1] | Satoe Numakura[1,2] | Hiroshi Uozaki[2] | Tetsuo Ushiku[1] | Masashi Fukayama[1,3] (iD)

[1]Department Pathology, Graduate School of Medicine, University of Tokyo, Tokyo, Japan

[2]Department Pathology, Teikyo University School of Medicine, Tokyo, Japan

[3]Asahi Telepathology Centre, Asahi General Hospital, Asahi, Japan

Correspondence
Masashi Fukayama, Department Pathology, Graduate School of Medicine, the University of Tokyo, Tokyo, Japan.
Email: mfukayama-tky@umin.org

Abstract

Cancer stem cells (CSCs) play a decisive role in the development and progression of cancer. To investigate CSCs in Epstein-Barr virus (EBV)-associated carcinoma (EBVaGC), we screened previously reported stem cell markers of gastric cancer in EBV-infected gastric cancer cell lines (TMK1 and NUGC3) and identified CD44v6v9 double positive cells as candidate CSCs. CD44v6/v9$^{+/+}$ cells were sorted from EBVaGC cell line (SNU719) cells and EBV-infected TMK1 cells and these cell populations showed high spheroid-forming ability and tumor formation in SCID mice compared with the respective CD44v6/v9$^{-/-}$ cells. Sphere-forming ability was dependent on the nuclear factor-κB (NF-κB) signaling pathway, which was confirmed by decrease of sphere formation ability under BAY 11-7082. Small interfering RNA knockdown of latent membrane protein 2A (LMP2A), one of the latent gene products of EBV infection, decreased spheroid formation in SNU719 cells. Transfection of the *LMP2A* gene increased the sphere-forming ability of TMK1 cells, which was mediated through NF-κB signaling. Together, these results indicate that CD44v6v9$^{+/+}$ cells are CSCs in EBVaGC that are maintained through the LMP2A/NF-κB pathway. Future studies should investigate CD44v6/v9$^{+/+}$ cells in normal and neoplastic gastric epithelium to prevent and treat this specific subtype of gastric cancer infected with EBV.

KEYWORDS
carcinoma, Epstein-Barr virus infection, neoplastic stem cell, signal transduction, stomach neoplasm

1 | INTRODUCTION

Epstein-Bar virus (EBV)-associated gastric carcinoma (EBVaGC), which involves monoclonal growth of EBV-infected epithelial cells,[1] is one of 4 molecular subtypes of gastric carcinoma[2] and accounts for 10% of total gastric carcinoma. The key abnormality of EBVaGC is an extremely high frequency of CpG-island methylation of the promoter region of various genes, including many cancer-associated genes.[1] However, the biological characteristics of EBVaGC have not been fully clarified.

Cancer stem cells (CSCs) possess the ability to induce tumor initiation and maintenance.[3] Candidate marker proteins of CSCs in gastric carcinoma include CD44 and its variant forms (CD44v6 and CD44v9), CD133, CD24, epithelial cell adhesion molecule (EpCAM),

LGR5, and ABCG2.[4] The gastric carcinoma subtypes are expected to show specific CSC markers, individually or in combination. However, no studies have examined the specific CSC markers or molecular mechanisms of maintaining CSCs in EBVaGC.

As EBVaGC is comprised of EBV-infected epithelial cells, an investigation into CSCs in EBVaGC needs 2 approaches. One approach is to identify cellular factors, such as essential signaling pathways, involved in the growth of CSCs. In nasopharyngeal carcinomas (NPC), another EBV-associated epithelial neoplasm,[5,6] nuclear factor-κB (NF-κB), Notch, PI3K/AKT, Hedgehog, and Wnt/β-catenin pathways all contribute to maintaining CSCs.[7-11] The second approach is to identify viral factors that could be involved in the growth of CSCs. A limited number of EBV-latent proteins are expressed in EBVaGC cells, such as EBV-determined nuclear antigen 1 and latent membrane protein 2A (LMP2A).[12] The latter plays an important role in transforming cancer cells, resulting in alteration of cell motility, inhibition of cell differentiation, and anchorage-independent cell growth. Together with LMP1, LMP2A also contributes to CSC development in NPC,[8,13] although LMP1 is rarely expressed in EBVaGC.[1]

In the present study, we identified both CD44v6 and CD44v9 as potential CSC markers in EBVaGC. We explored the molecular mechanism of CSC maintenance using these CSC markers of EBVaGC.

2 | MATERIALS AND METHODS

The research project was approved by the Ethics Committee of the Graduate School of Medicine, University of Tokyo, and the work was undertaken and conforms to the provisions of the Declaration of Helsinki.

2.1 | Cell culture

The gastric cancer cell lines, NUGC3 (Japanese Cancer Research Resource Center, Osaka, Japan) and TMK1 (Professor Wataru Yasui, Hiroshima University, Hiroshima, Japan), were established from human gastric carcinoma with histologic features of poorly differentiated adenocarcinoma. SNU719 (Korean Cell Line Bank, Seoul, South Korea) and YCCEL1 cells (Professor Sun Young Rha, Yonsei University, Seoul, South Korea) were derived from EBVaGC. NUGC3, TMK1, and SNU719 cells were maintained in RPMI-1640 (Nacalai Tesque), supplemented with 10% FBS (Sigma-Aldrich) and 5% penicillin-streptomycin (Nacalai Tesque). YCCEL1 cells were maintained in MEM (Nacalai Tesque).

2.2 | Epstein-Barr virus infection

Using the cell-to-cell contact method, NUGC3 and TMK1 cells were infected with recombinant EBV through the Akata cell line (gift from Professor K Takada, Hokkaido University). Both EBV-infected cell lines (EBV⁺ NUGC3 and EBV⁺ TMK1, respectively) were selected and maintained with 800 μg/mL G418 (Roche Diagnostics).

2.3 | RNA interference

Small interfering RNA directed against LMP2A (5′-AACUCCCAAUAUCCAUCUGCUUU-3′) was custom synthesized and purchased from Dharmacon (ON-TARGET siRNA). siGENOME Non-Targeting siRNA pool #1 was used as negative control (D-001206-13-20; Dharmacon). SNU719 cells were transfected with siRNAs, siLMP2A, and siControl at 5 nmol/L by transfection reagent Lipofectamine RNAiMAX (Thermo Fisher Scientific) according to the manufacturer's instructions. RNA was collected at 48 hours after each siRNA was transfected. Spheroid number and diameter were measured 7 days after each siRNA was transfected.

2.4 | Plasmids and transfection

Latent membrane protein 2A cDNA (a gift from Professor Paul J. Farrell, Imperial College of London) was cloned into pcDNA3.1 to generate pcDNA3.1-LMP2A. The empty pcDNA3.1 vector containing FLAG-tag (pcDNA3.1-FLAG) was used as a control. Transfection was carried out using Lipofectamine 3000 reagent (Thermo Fisher Scientific) according to the manufacturer's protocol. Pooled TMK1 cell populations expressing pcDNA3.1-LMP2A or pcDNA3.1-FLAG were selected with 800 μg/mL G418.

2.5 | Flow cytometry analysis and cell sorting

Cells were washed once with PBS and dissociated from plates with Accutase (Nacalai Tesque). Cells were centrifuged and resuspended with PBS (1×10^5–1×10^6 cells/100 μL). Cells were incubated at 4°C in the dark for 30 minutes and labeled with the following primary-conjugated Abs: CD44-phycoerythrin (PE) (DB105), CD133-FITC (AC133), CD24-FITC (32D12), EpCAM-FITC (HEA-125), LGR5-PE (DA03-22H2.8), and ABCG2-FITC (5D3) (Miltenyi Biotec). CD44v6 (VFF-18; Abcam) and CD44v9 (RV3; Cosmo Bio) were used after labeling with secondary PE (BD Biosciences) and Alexa Fluor 488 (Thermo Fisher Scientific), respectively. Approximately 1-3 × 10⁴ cells were analyzed with a BD LSR Fortessa flow cytometer (BD Biosciences). Isotypic IgG and unstained cells served as negative control. For cell sorting, 1×10^7–1×10^8 cells were collected and stained with CD44v6 and CD44v9. The stained cells were then sorted into CD44v6/v9⁺/⁺ and CD44v6/v9⁻/⁻ populations using the Moflo XDP cell sorter (Beckman Coulter).

2.6 | Spheroid formation assay

A total of 500-10 000 cells were seeded in each well of ultra-low attachment 96-well plates (Corning Life Sciences) supplemented with 100 μL serum-free medium (either RPMI-1640 or MEM depending on the cell line), 10 mmol/L HEPES (Thermo Fisher Scientific), 20 ng/mL human recombinant epidermal growth factor (Wako), 10 ng/mL human
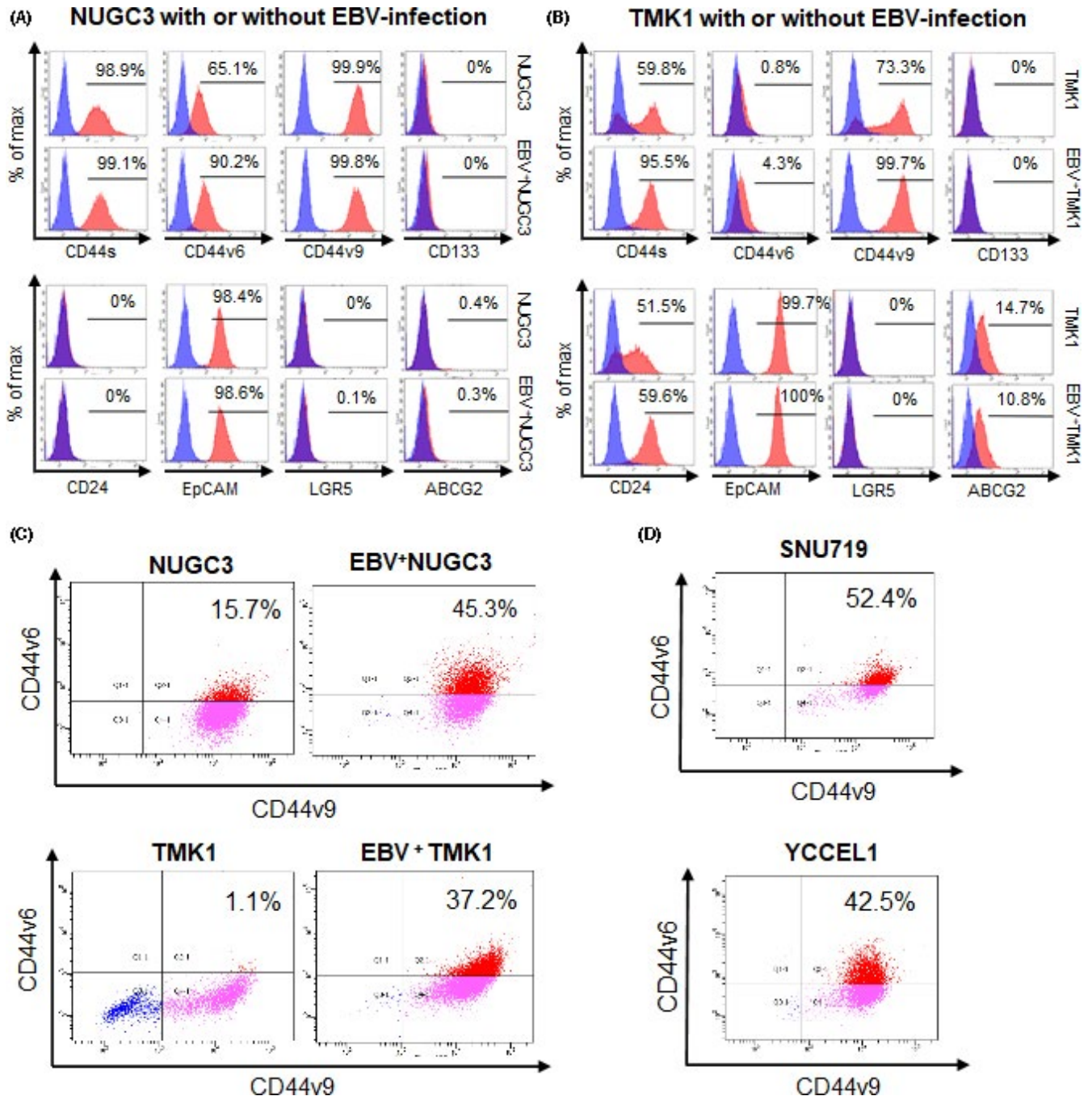
FIGURE 1 Cancer stem cell markers in gastric cancer cell lines experimentally or naturally infected with Epstein-Barr virus (EBV). A, FACS analysis of cancer stem cell markers in NUGC3 gastric cancer cells with and without EBV infection. Isotype control is indicated as a blue peak. The percentage of the positive fraction is shown in each graph. B, FACS analysis of cancer stem cell markers in TMK1 gastric cancer cells with and without EBV infection. C, Dual color analysis of CD44v6 and CD44v9 expression in NUGC3 and TMK1 gastric cancer cells with and without EBV infection. Horizontal axis, Alexa Fluor488-CD44v9; vertical axis, phycoerythrin (PE)-CD44v6. D, Dual color analysis of CD44v6 and CD44v9 expression in EBV-associated gastric carcinoma cell lines SNU719 and YCCEL1. Horizontal axis, Alexa Fluor 488-CD44v9; vertical axis, PE-CD44v6

recombinant basic fibroblast growth factor (Wako), 1% N-2 supplement (Thermo Fisher Scientific), 2% B-27 supplement (Thermo Fisher Scientific), and 5% penicillin-streptomycin (Nacalai Tesque). After 7-14 days, each well was examined with a light microscope; the number of spheroid colonies with a diameter more than 50 μm was counted. The diameter of each spheroid colony was also measured.

2.7 | Spheroid formation assay with inhibitors

Assays were carried out using the NF-κB inhibitor (BAY 11-7082), PI3K inhibitor (LY 294002), and the γ secretase inhibitor IX, DAPT (Calbiochem, Merck Millipore) used to block Notch signaling. Stock solutions of the inhibitors were prepared by diluting in DMSO to a

concentration of 100 mmol/L. Inhibitors were added to cells every 2 days.

2.8 | In vivo tumorigenicity experiment

Mice (SCID, 4-5 weeks of age) were purchased from Charles River Laboratories Japan. A total of 90 000 cells of CD44v6/v9$^{+/+}$ and CD44v6/v9$^{-/-}$ cells from SNU719 cells were suspended in 100 μL PBS with 50% Matrigel and injected s.c. into the flank of SCID mice (n = 10 per group). In other experiments, a total of 150 000 EBV$^+$ TMK1 cells were used for tumorigenic experiments in SCID mice (n = 5 per group). The tumor diameter was measured twice a week, and the tumor volume (v) was calculated according to the following equation: v (mm^3) = length × width^2/2. The mice were killed, and the tumors were removed 67 days or 34 days after injection for SNU719 cells or EBV$^+$ TMK1 cells, respectively. All mice were given adequate humanitarian care in accordance with both NIH animal protection organization guidelines and the institutional guidelines.

2.9 | Microarray analysis

SNU719 cells were subjected to oligonucleotide microarray analysis. Total RNA was extracted from monolayer and sphere-forming SNU719 cells. SurePrint G3 Human GE Microarray 8 × 60K v3 (Agilent Technologies) was scanned on an Agilent Microarray Scanner. The data were normalized and analyzed with GeneSpring GX (Agilent Technologies). The upregulated genes (4-fold change or more) were subjected to Gene Ontology analysis using Gene Ontology term database in the DAVID functional annotation tool version 6.8 (https://david.ncifcrf.gov).

2.10 | Western blot analysis

Cells were washed in PBS and centrifuged. Nuclear extracts were isolated using NE-PER nuclear and cytoplasmic extraction reagents, according to the manufacturer's instructions (Thermo Fisher Scientific). The nuclear extracts were applied to SDS-PAGE and immunoblot analysis. The following Abs were used: anti-p65 (relA) Ab (D14E12; Cell Signaling Technology) and anti-histone H3 Ab (ab1791; Abcam). Band intensity was quantified using Image Lab (Bio-Rad) and then normalized with histone H3. The relative band intensity was expressed as fold change as compared to control.

2.11 | Reverse transcription-PCR of LMP2A

Total RNA was extracted from gastric cancer cells using ISOGENII (Nippon Gene, Tokyo, Japan). Total RNA (0.5 μg) was used for cDNA synthesis with ReverTra Ace qPCR RT Kit (Toyobo). The

mRNA levels were measured by a Thermal Cycler Dice Real Time System (TaKaRa) and KAPA SYBR Fast qPCR Kit (Kapa Biosystems). The following primers were used for PCR: LMP2A primer forward, 5′-ATGACTCATCTCAACACATA-3′ and reverse, 5′-CATGTTAGGCAAATTGCAAA-3′; and GAPDH primer forward, 5′-GAAGGTGAAGGTCGGAGTC-3′ and reverse, 5′-GAAGATGGTGATGGGATTT-3′. The fold changes of the gene expression were calculated by the $2^{-\Delta\Delta CT}$ method.

2.12 | Statistical analysis

Data are expressed as mean ± SD. Mann-Whitney U test and Dunnett's test were carried out using GraphPad Prism version 6.0 (GraphPad Software). P less than .05 was considered statistically significant.

3 | RESULTS

### 3.1 | Identification of CSC markers in EBVaGC cell lines

To identify stem-like subpopulations in EBVaGC cells, we analyzed the expression of multiple cell surface markers in NUGC3 and TMK1 gastric cancer cell lines with or without EBV infection by flow cytometry. We observed increased CD44v6 in EBV$^+$ NUGC3 cells and CD44s, CD44v6, and CD44v9 in EBV$^+$ TMK1 cells compared with the respective original cell lines (Figure 1A,B).

Based on these findings, we evaluated CD44v6/v9$^{+/+}$double positive fractions in both gastric cancer cell lines with and without EBV infection. CD44v6/v9$^{+/+}$ cells were increased in EBV$^+$ NUGC3 and EBV$^+$ TMK1 cells compared with the respective original cells (Figure 1C). Double positive fractions were enriched in the naturally EBV-infected gastric cancer cell lines SNU719 and YCCEL1 (Figure 1D). These findings suggested that CD44v6/v9$^{+/+}$ components were candidates CSCs in EBVaGC.

3.2 | Spheroid formation in CD44v6/v9$^{+/+}$ EBV-infected gastric cells

Preliminary experiments showed that SNU719 and EBV$^+$ TMK1 cells formed discrete spheroids, but YCCEL1 or EBV$^+$ NUGC3 did not (data not shown). Therefore, SNU719 and EBV$^+$ TMK1 cells were used for quantitative comparison.

Compared with TMK1 cells, EBV$^+$ TMK1 cells showed increased spheroid formation (EBV$^+$ TMK1 vs. TMK1 cells, 54.2 ± 10.1 vs. 31.2 ± 10.5 colonies, P < .0001) with a larger diameter size (P = .0407) (Figure 2A).The CD44v6/v9$^{+/+}$and CD44v6/v9$^{-/-}$ fractioned SNU719 and EBV$^+$ TMK1 cells were subjected to spheroid formation assay (Figures 2B,C and S1). The number of spheroid colonies was significantly higher in CD44v6/v9$^{+/+}$ sorted cells than

(A) TMK1 EBV⁺TMK1

(B) SNU719

(C) EBV⁺TMK1
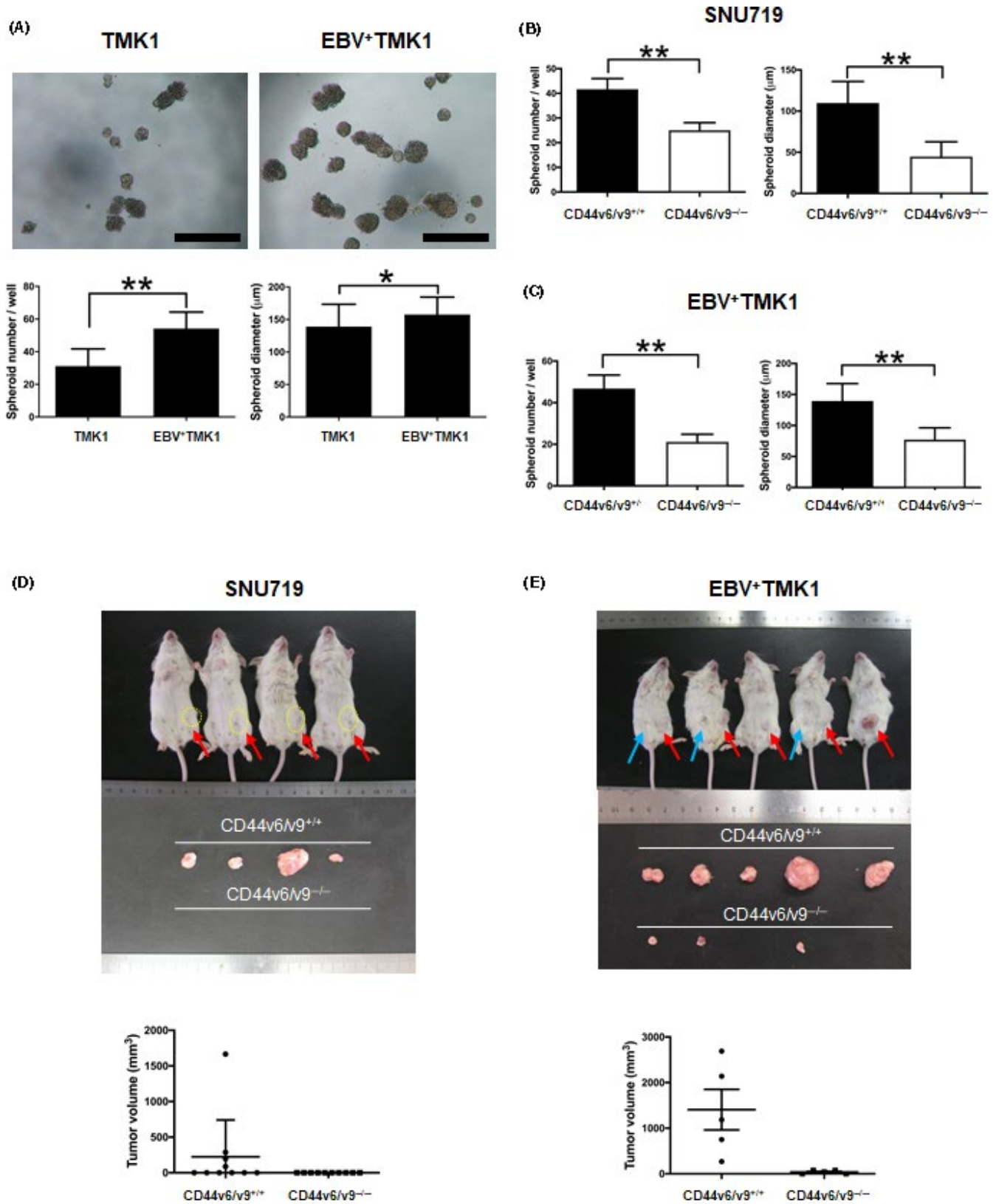
(D) SNU719

(E) EBV⁺TMK1

CD44v6/v9⁻/⁻ sorted cells in SNU719 cells (41.6 ± 4.3 vs. 25.0 ± 3.1 colonies, P = .0002) and EBV⁺ TMK1 cells (46.8 ± 6.5 vs. 21.1 ± 3.7 colonies, P = .0002), respectively. The diameter of the spheroid colonies was significantly larger in CD44v6/v9⁺/⁺ fractioned cells than in CD44v6/v9⁻/⁻ fractioned cells in SNU719 (P < .0001) and EBV⁺ TMK1 cells (P < .0001).

FIGURE 2 Cancer stem cells in Epstein-Barr virus (EBV)-associated gastric cancer are enriched for CD44v6/v9$^{+/+}$ cells. A, Spheroid formation ability of TMK1 and EBV$^+$ TMK1 cells. Upper panels, representative images of spheroid colonies derived from TMK1 and EBV$^+$ TMK1 cells (7 days). Lower panels, number and diameter of the spheres (mean ± SD; **$P < .01$, Mann-Whitney U test). B, Spheroid formation assay of CD44v6/v9$^{+/+}$ and CD44v6/v9$^{-/-}$ fractioned cells of SNU719 cells. A total of 10 000 cells were seeded in each well. Measurement of the number (left) and diameter (right) of spheroid colonies after 10 days (mean ± SD; *$P < .05$, **$P < .01$, Mann-Whitney U test). C, Spheroid formation assay of CD44v6/v9$^{+/+}$ and CD44v6/v9$^{-/-}$ fractioned cells of EBV$^+$ TMK1 cells. A total of 500 cells were seeded in each well. Measurement of the number (left) and diameter (right) of spheroid colonies after 10 days (mean ± SD; *$P < .05$, **$P < .01$, Mann-Whitney U test). D, Tumor formation of CD44v6/v9$^{+/+}$ and CD44v6/v9$^{-/-}$ cells from SNU719 cells in vivo. A total of 90 000 cells embedded in Matrigel were inoculated s.c. into SCID mice (n = 10 per group). Measurement of the tumor volume after 67 days (red arrows indicate tumors derived from CD44v6/v9$^{+/+}$ cells). Lower graph shows volume (mean ± SEM). E, Tumor formation of CD44v6/v9$^{+/+}$ and CD44v6/v9$^{-/-}$ cells from EBV$^+$ TMK1 in vivo. A total of 150 000 cells embedded in Matrigel were inoculated s.c. into SCID mice (n = 5 per group). Measurement of tumor volumes after 34 days (blue arrows indicate tumors derived from CD44v6/v9$^{-/-}$ cells, and red arrows indicate tumors derived from CD44v6/v9$^{+/+}$ cells). Lower graph shows tumor volume (mean ± SEM; $P = .0079$, Mann-Whitney U test)

3.3 | CD44v6/v9$^{+/+}$ fractioned cells show high tumor-initiating ability in vivo

The SCID mice were s.c. inoculated with CD44v6/v9$^{+/+}$ and CD44v6/v9$^{-/-}$ sorted cells. CD44v6/v9$^{+/+}$ SNU719 cells produced palpable tumors 67 days after inoculation in 4 out of 10 mice (Figure 2D); CD44v6/v9$^{-/-}$ SNU719 cells did not generate any tumors. CD44v6/v9$^{+/+}$ EBV$^+$ TMK1 cells formed large palpable tumors 34 days after inoculation in all mice, whereas CD44v6/v9$^{-/-}$ EBV$^+$ TMK1 cells produced small-sized tumors only in 3 out of 5 mice ($P = .0079$) (Figure 2E). Cancer stem cells retain the capability to differentiate to mature cells. To evaluate the fate of CD44v6/CD44v9$^{+/+}$ cells in the xenografts, the excised tumors were analyzed by immunohistochemistry and flow cytometry (Figure S2). These analyses confirmed some differentiation in the transplanted tumors.

3.4 | Signaling pathways involved in spheroid formation of EBVaGC cells

To identify a candidate pathway involved in enhancing stemness of EBVaGC, oligonucleotide microarray analysis was carried out to compare gene expression between monolayer and sphere-forming SNU719 cells. Among the signaling pathways that were previously reported to be involved in NPC [7-11] (TableS1), NF-κB ($P=.029$), Notch ($P=.045$), and PI3K/AKT ($P=.045$) pathways were identified as significantly upregulated pathways in spheroids of SNU719 cells. Spheroid assays were undertaken using SNU719 and EBV$^+$ TMK1 cells with BAY 11-7082 (NF-κB inhibitor), DAPT (Notch inhibitor), and LY294002 (PI3K/AKT inhibitor). In SNU719 cells, the number and diameter of tumor spheres were significantly decreased with BAY 11-7082 treatment (Figure 3 A). In EBV$^+$ TMK1 cells, both spheroid number and diameter were significantly decreased under BAY 11-7082 treatment (Figure 3B). The effect of DAPT was not significant in reducing spheroid number or spheroid diameter in either cell type except at a concentration of 5μmol/L DAPT in EBV$^+$ TMK1 cells (Figure 3C,D). LY294002 showed an inhibitory effect on the spheroid number and diameter in SNU719 and EBV$^+$ TMK1 cells at 50μmol/L (Figure 3E,F).

3.5 | Latent membrane protein 2A contributes to cancer stemness in EBVaGC cells

To evaluate the contribution of a viral latent protein, LMP2A, to the stemness of EBVaGC, we compared LMP2A expression in monolayer and sphere-forming cells of both SNU719 and EBV$^+$ TMK1 lines by RT-PCR analysis (Figure 4A,B). We found a 4.8-fold and a 4.1-fold increase in spheroid cells, respectively.

When LMP2A expression was knocked down with siRNA (Figure S3A), both the number and diameter of spheroids significantly decreased (Figure 4C,D). Next, we transfected pcDNA3.1-LMP2A and pcDNA3.1-Flag into TMK1 cells to generate LMP2A$^+$ TMK1 and Flag$^+$ TMK1 cells, respectively (Figure S3B). The LMP2A$^+$ TMK1 cells produced significantly more spheroids with larger diameter than Flag$^+$ TMK1 cells (Figure 4E,F, $P < .01$).

3.6 | Latent membrane protein 2A/NF-κB pathway in cancer stemness of EBVaGC cells

To evaluate the possibility that LMP2A promotes cancer stemness through activation of NF-κB signaling, we undertook western blotting of its downstream factor, p65, which revealed a 1.86-fold increase in LMP2A$^+$ TMK1 compared with Flag$^+$ TMK1 cells (Figure 5A).

Next, we compared the inhibitory effect of NF-κB signaling on the spheroid-forming ability of LMP2A$^+$ TMK1 (Figure 5B) with that of EBV$^+$ TMK1 cells. In the comparison of EBV$^+$ TMK1 with TMK1, the number of spheroid colonies of EBV$^+$ TMK1 cells steeply decreased in response to BAY 11-7082 in a dose-dependent manner. The number of the colonies increased in TMK1 cells with 1μmol/L BAY 11-7082 and then decreased with concentrations of 2.5μmol/L and 5μmol/L. In the comparison of LMP2A$^+$ TMK1 with Flag$^+$ TMK1 cells, the effect of BAY 11-7082 on sphere formation was greater in LMP2A$^+$ TMK1 than in Flag$^+$ TMK1 cells (Figure 5C,D). Then the inhibitory effect of BAY 11-7082 was compared between EBV$^+$ TMK1 and LMP2A$^+$ TMK1 cells by plotting each observed ratio to the control ratio (Figure 5E,F). We observed an increase of 1.8-fold in the number of spheroid colonies in EBV$^+$ TMK1 relative to TMK1
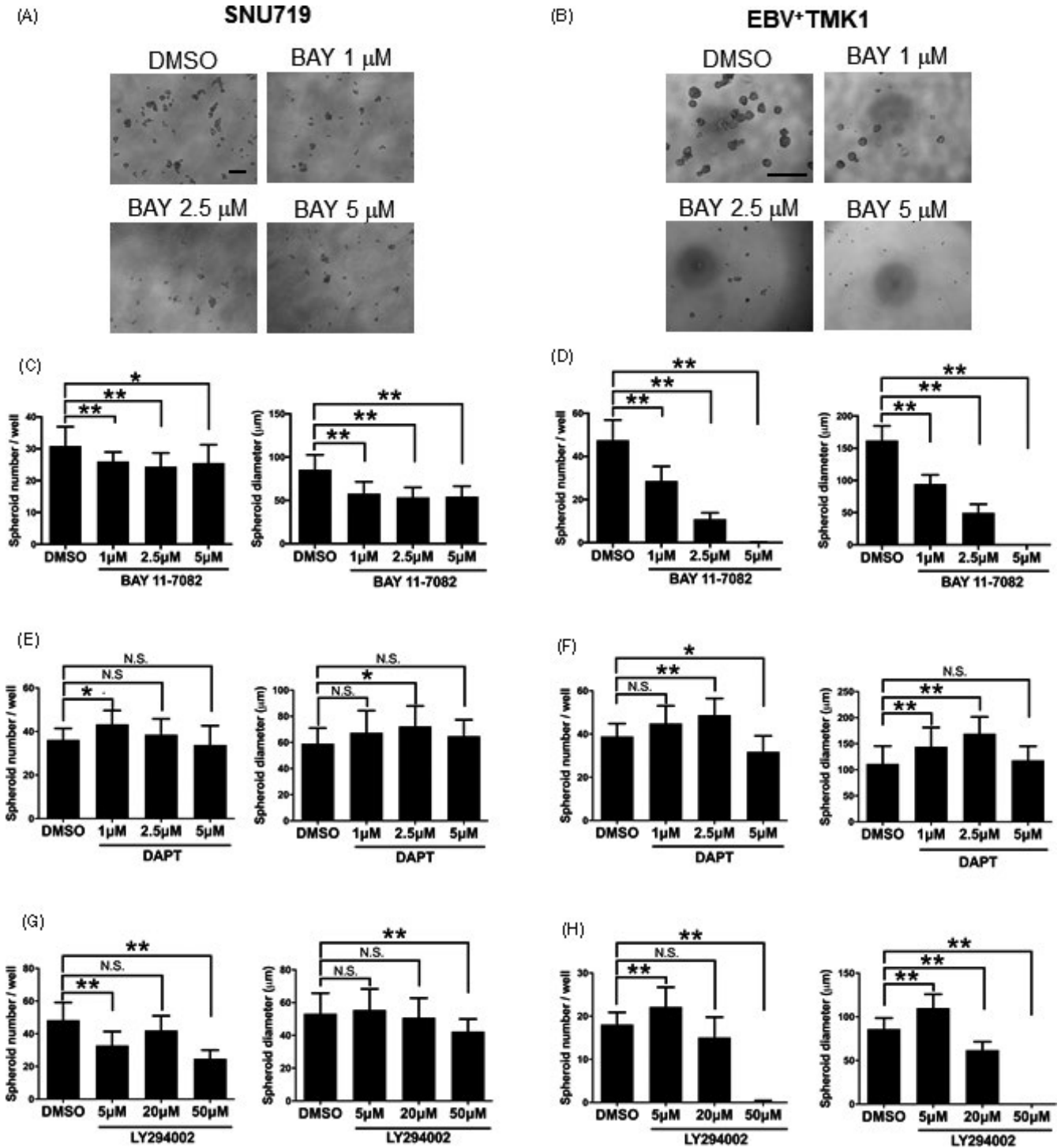
FIGURE 3 Nuclear factor-κB (NF-κB) pathway contributes to maintenance of cancer stem cells in Epstein-Barr virus (EBV)-associated gastric cancer. A, Spheroid formation assay of SNU719 cells treated with the NF-κB inhibitor, BAY 11-7082 (1, 2.5, or 5μmol/L). A total of 10000 cells were seeded in each well. Measurement of the number (left graph) and diameter (right graph) of spheroid colonies after 7days. B, Spheroid formation assay of EBV⁺ TMK1 cells treated with the NF-κB inhibitor, BAY 11-7082 (1, 2.5, or 5μmol/L). A total of 500 cells were seeded in each well. Measurement of the number (left graph) and diameter (right graph) of spheroid colonies after 7days. C, E, Spheroid formation assay in SNU719 cells treated with the Notch inhibitor (γ secretase inhibitor IX, DAPT) (1, 2.5, or 5μmol/L) (C) or PI3K inhibitor LY294002 (5, 20, or 50μmol/L) (E). A total of 10000 cells were seeded in each well. Measurement of the number (left) and diameter (right) of spheroid colonies after 7days. D, F, Spheroid formation assay of EBV⁺ TMK1 cells treated with Notch inhibitor (γ secretase inhibitor IX, DAPT) (1, 2.5, or 5μmol/L) (D) or PI3K inhibitor LY294002 (5, 20, or 50μmol/L) (F). A total of 500 cells were seeded in each well. Measurement of the number (left) and diameter (right) of spheroid colonies after 7days. All data are shown as mean±SD; *$P<.05$, **$P<.01$, Dunnett's test. N.S., not statistically significant

FIGURE 4 Latent membrane protein 2A (LMP2A) plays an important role in maintenance of cancer stem cells in Epstein-Barr virus (EBV)-associated gastric cancer. A and B, Relative mRNA expression of LMP2A in monolayer cells (2D) and sphere-forming cells (spheroid) of SNU719 and EBV⁺ TMK1 cells, respectively. C and D, Effects of LMP2A knockdown on spheroid formation of SNU719 cells, respectively. A total of 10 000 cells were seeded in each well. Measurement of the number (C) and diameter (D) of spheroid colonies after 7 days. E and F, Effects of LMP2A transfection on spheroid formation of TMK1 cells. A total of 500 cells were seeded in each well. Measurement of the number (E) and diameter (F) of spheroid colonies after 7 days (left). All data are shown as mean ± SD; **$P < .01$, Mann-Whitney U test
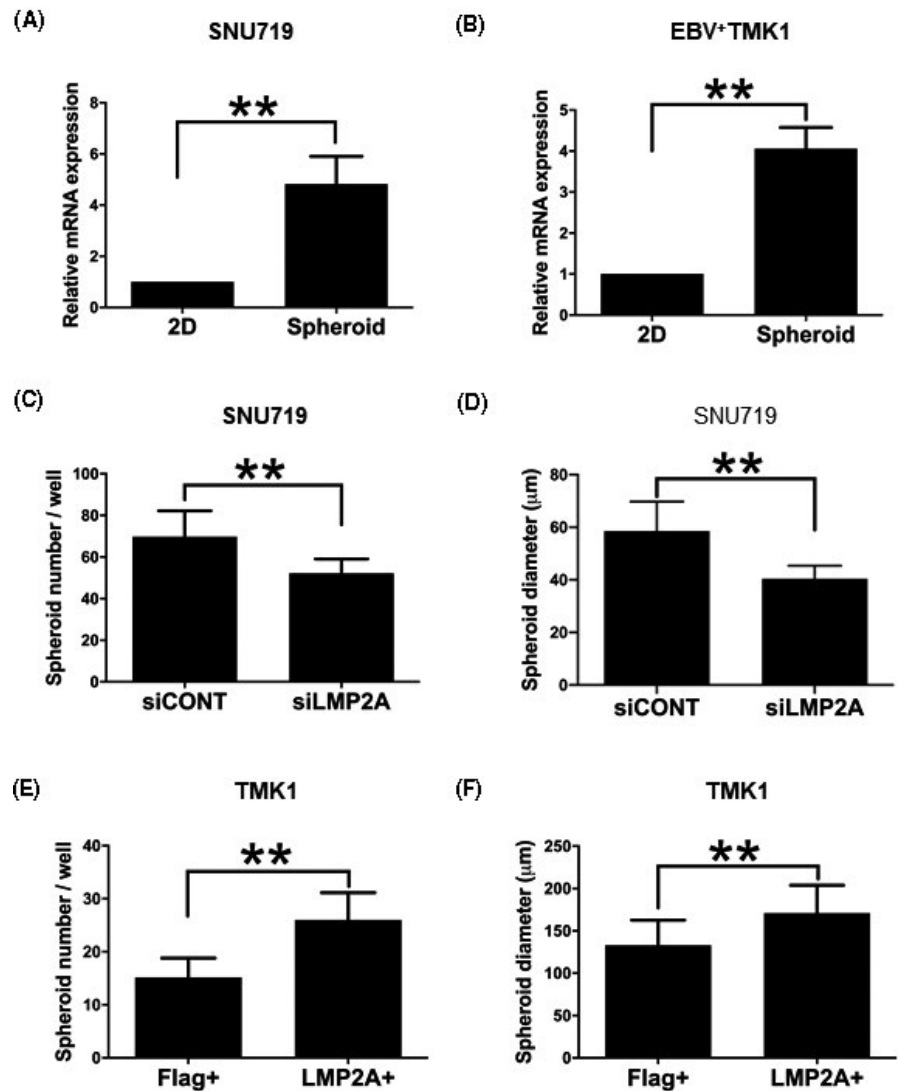
cells and an increase of 1.4-fold in LMP2A⁺ TMK1 relative to Flag⁺ TMK1 cells. The fold decrease in sphere formation in response to BAY 11-7082 was similar between both cell lines at concentrations of 1μmol/L and higher.

4 | DISCUSSION

No studies have previously investigated CSCs in EBVaGC. In the present study, we first identified 2 potential CSC markers of EBVaGC, CD44v6, and CD44v9. CD44 is the major cell surface receptor for hyaluronate and has been implicated in several cellular mechanisms, including lymphocyte homing. The *CD44* gene consists of 20 exons; the CD44s variant, which comprises the first and last 5 exons, is ubiquitously expressed. The central 10 exons undergo extensive alternative splicing to generate splicing variants (CD44v isoforms) that are variably expressed in cancer cells and CSCs.[14] In the present study, we found that CSCs were enriched for CD44v6/v9⁺/⁺ cells among EBV⁺ TMK1 cells and the SNU719 EBVaGC cell line. CD44v9

is a CSC marker in various kinds of solid tumors, including gastric cancer. CD44v9 stabilizes the glutamate-cystine transporter xCT on the cytoplasmic membrane, thereby decreasing intracellular reactive oxygen species.[15] CD44v6 is also a CSC marker in various types of cancer, such as colon cancers,[16] in which binding of hepatocyte growth factor (HGF) with CD44v6 induces Ras signaling activation through the CD44v6/HGF/cMet complex.[17]

Spheroid-forming cells show enriched stem cell properties compared with the whole tumor mass or unselected monolayer cells. In the present study, we applied this distinction to identify the signaling pathway for the maintenance of stemness in EBVaGC. Comparison of the expression profiles between spheroid and monolayer culture of SNU719 EBVaGC cells identified NF-κB, Notch, and PI3K/AKT signaling pathways as candidates among pathways reported in NPC.[7-11] We found that the NF-κB pathway is the most significant contributor to stem cell properties in EBVaGC using spheroid formation experiments with specific inhibitors. Nuclear factor-κB is constitutively activated in EBVaGC[18] and serves as a resisting factor to serum-deprivation-induced
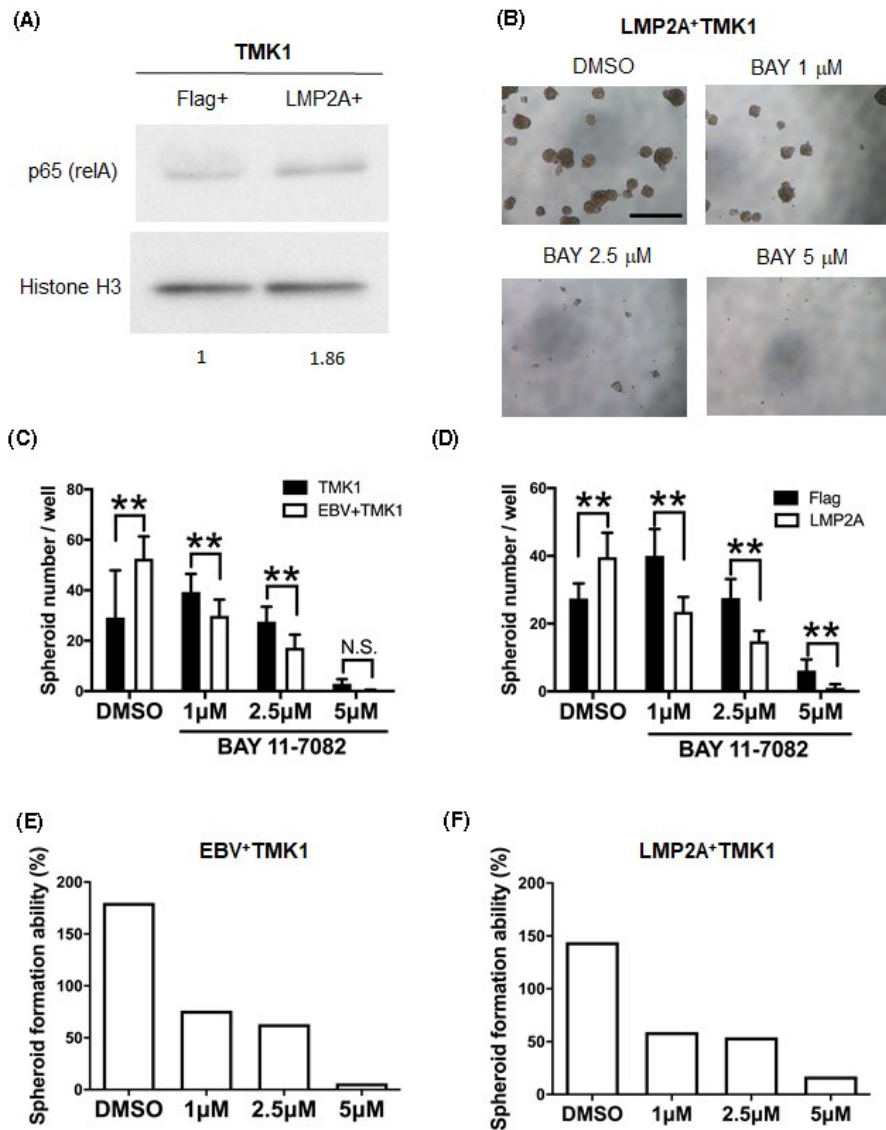
FIGURE 5 Effect of latent membrane protein 2A (LMP2A) on stem cell properties is mediated through the nuclear factor-κB (NF-κB) pathway. A, Western blot of p65 (relA) and histone H3 in TMK1 cells transfected with Flag- and LMP2A-containg vectors. Relative expression of p65 to histone H3 is 1.86-fold higher in LMP2A^{+} TMK1 than in Flag[+] TMK1. B, Spheroid formation ability of LMP2A-transfected TMK1 cells (LMP2A^{+} TMK1) treated with BAY 11-7082 (1, 2.5, or 5μmol/L). Representative images are shown. C and D, Spheroid formation ability of LMP2A^{+} TMK1 and Flag^{+} TMK1 cells treated with BAY 11-7082 (1, 2.5, or 5μmol/L), respectively. A total of 500 cells were seeded in each well. Measurement of the number of spheroid colonies after 7days (left) (mean±SD; **P<.01, Mann-Whitney U test; N.S., not statistically significant). E, Relative proportions of spheres in EBV^{+} TMK1 cells to TMK1 cells at each concentration. F, Relative proportions of spheres in LMP2A^{+} TMK1 cells to Flag[+]TMK1 cells at each concentration

apoptosis through upregulation of survivin.[12] However, further studies are necessary to clarify the role of NF-κB in the maintenance of stemness or CSCs in EBVaGC.

Nuclear factor-κB signaling is activated in inflammation-associated neoplasms, but the mechanisms of upregulation are dependent on the organ, inflammation, and infective agent. To identify the mechanisms of NF-κB upregulation in EBVaGC, we evaluated the contribution of the viral protein, LMP2A. Latent membrane protein 2A is involved in enhancing CSCs in NPC,[13] which we confirmed in EBVaGC cells (SNU719) by siRNA inhibition. In the present study, we also transfected LMP2A to TMK1 cells, showing that the LMP2A-induced increase of sphere formation was dependent on NF-κB in TMK1 cells. As the increase of sphere formation ability of TMK1 cells was slightly lower than that of EBV-infected TMK1 cells, it is possible that other latent gene products, such as EBNA1 or noncoding RNAs, play an additional role in CSC maintenance.

Cancer stem cells could also share many properties with tumor-initiating cells of non-neoplastic epithelium. In stomach mucosa infected with *Helicobacter pylori*, CD44v9 is induced in cells overexpressing CAPZA, a negative regulator of autophagy, after accumulation of cytotoxin associated gene A (CagA),[19] which exerts its growth promotion effect through activation of the SHP2 tyrosine phosphatase. Its homologue, SHP1 antagonizes CagA and is downregulated by CpG-island methylation in EBVaGC.[20] These facts suggest that CD44v6/v9^{+/+} epithelial cells, induced by *H. pylori* infection, might be a precursor of EBVaGC.

In conclusion, we found that CSC properties were enriched in the CD44v6/v9^{+/+} fraction of cancer cells, suggesting that CD44v6/v9 is a unique CSC marker for EBVaGC. Sphere formation ability was induced through the LMP2A-NFκB pathway, and this pathway could be a potential therapeutic target for EBVaGC.

ACKNOWLEDGMENTS

Technology Agency to MF. We thank Edanz Group for editing a draft of this manuscript.

CONFLICT OF INTEREST

ORCID

Masashi Fukayama https://orcid.org/0000-0002-0460-064X

REFERENCES

1. FukayamaM, KunitaA, KanedaA. Gastritis-infection-cancer sequence of Epstein-Barr virus-associated gastric cancer. *Adv Exp Med Biol.* 2018;1045:437-457.
2. The Cancer Genome Atlas Research Network. Comprehensive molecular characterization of gastric adenocarcinoma. *Nature.* 2014;513:202-209.
3. NguyenLV, VannerR, DirksP, et al. Cancer stem cells: an evolving concept. *Nat Rev Cancer.* 2012;12:133-143.
4. SongY, WangY, TongC, et al. A unified model of the hierarchical and stochastic theories of gastric cancer. *Br J Cancer.* 2017;116:973-989.
5. LunS-M, CheungST, CheungPFY, et al. CD44+ Cancer stem-like cells in EBV-associated nasopharyngeal carcinoma. *PLoS ONE.* 2012;7:e52426.
6. HoeSLL, TanLP, Abdul AzizN, et al. CD24, CD44 and EpCAM enrich for tumour-initiating cells in a newly established patient-derived xenograft of nasopharyngeal carcinoma. *Sci Rep.* 2017;7:12372.
7. LiaoK, XiaB, ZhuangQY, et al. Parthenolide inhibits cancer stem-like side population of nasopharyngeal carcinoma cells via suppression of the NF-κB/COX-2 pathway. *Theranostics.* 2015;5:302-321.
8. YangC-F, YangG-D, HuangT-J, et al. EB-virus latent membrane protein 1 potentiates the stemness of nasopharyngeal carcinoma via preferential activation of PI3K/AKT pathway by a positive feedback loop. *Oncogene.* 2016;35:3419-3431.
9. CheungC-M, LunS-M, ChungG-Y, et al. MicroRNA-183 suppresses cancer stem-like cell properties in EBV-associated nasopharyngeal carcinoma. *BMC Cancer.* 2016;16:495.
10. PortRJ, Pinheiro-MaiaS, HuC, et al. Epstein-Barr virus induction of the Hedgehog signalling pathway imposes a stem cell phenotype on human epithelial cells. *J Pathol.* 2013;231:367-377.
11. ChanKC, ChanLS, ChokJ, et al. Therapeutic targeting of CBP/β-catenin signaling reduces cancer stem-like population and synergistically suppresses growth of EBV-positive nasopharyngeal carcinoma cells with cisplatin. *Sci Rep.* 2015;5:9979.
12. Shinozaki-UshikuA, KunitaA, FukayamaM. Update on Epstein-Barr virus and gastric cancer (review). *Int J Oncol.* 2015;46:1421-1434.
13. KongQ-L, HuL-J, CaoJ-Y, et al. Epstein-Barr virus-encoded LMP2A induces an epithelial- mesenchymal transition and increases the number of side population stem-like cancer cells in nasopharyngeal carcinoma. *PLoS Pathog.* 2010;6:e1000940.
14. YanY, ZuoX, WeiD. Concise Review: Emerging role of CD44 in cancer stem cells: A promising biomarker and therapeutic target. *Stem Cells Transl Med.* 2015;4:1033-1043.
15. IshimotoT, NaganoO, YaeT, et al. CD44 variant regulates redox status in cancer cells by stabilizing the xCT subunit of system xc(-) and thereby promotes tumor growth. *Cancer Cell.* 2011;19:387-400.
16. TodaroM, GaggianesiM, CatalanoV, et al. CD44v6 is a marker of constitutive and reprogrammed cancer stem cells driving colon cancer metastasis. *Cell Stem Cell.* 2014;14:342-356.
17. Orian-RousseauV, ChenL, SleemanJP, et al. CD44 is required for two consecutive steps in HGF / c-Met signaling. *Genes Dev.* 2002;16:3074-3086.
18. ZhangY, LiuW, ZhangW, et al. Constitutive activation of the canonical NF-κB signaling pathway in EBV-associated gastric carcinoma. *Virology.* 2019;532:1-10.
19. TsugawaH, KatoC, MoriH, et al. Cancer stem-cell marker CD44v9-positive cells arise from Helicobacter pylori-infected CAPZA1-overexpressing cells. *Cell Mol Gastroenterol Hepatol.* 2019;8:319-334.
20. SajuP, Murata-KamiyaN, HayashiT, et al. Host SHP1 phosphatase antagonizes *Helicobacter pylori* CagA and can be downregulated by Epstein-Barr virus. *Nat Microbiol.* 2016;1:16026.

SUPPORTING INFORMATION

Additional supporting information may be found online in the Supporting Information section.